CHEMISTRY
A EUROPEAN JOURNAL

DOI: 10.1002/chem.201001181

Metal–Molecule–Metal Junctions in Langmuir–Blodgett Films Using a New Linker: Trimethylsilane

Gorka Pera,[a, b] Santiago Martín,[a, b] Luz M. Ballesteros,[a, b] Adam J. Hope,[c] Paul J. Low,[c] Richard J. Nichols,[d] and Pilar Cea*[a, b]

Abstract: Herein trimethylsilane (TMS) is demonstrated to be an efficient binding group suitable for construction of metal–molecule–metal (M–mol–M′) junctions, in which one of the metal contacts is an atomically flat gold surface and the other a scanning tunnelling microscopy (STM) tip. The molecular component of the M–mol–M′ devices is an oligomeric phenylene ethynylene (OPE) derivative Me_3Si C≡C{C_6H_4C≡C}$_2C_6H_4NH_2$, featuring both Me_3SiC≡C and NH_2 metal contacting groups. This compound can be assembled into Langmuir–Blodgett (LB) films on Au−substrates by surface binding through the amine groups. Alternatively, low coverage (sub-monolayer) films are formed by adsorption from solution. In the case of condensed monolayers top electrical contacts are formed to STM tips through the TMS end group. In low coverage films, single molecular bridges can be formed between the gold surface and a gold STM tip. The similarity in the *I–V* response of a one-layer LB film and the single molecule conductance experiments reveals several points of critical importance to the design of molecular components for use in the construction of M–mol–M′ junctions. Firstly, the presence of neighbouring π systems does not have a significant effect on the conductance of the M–mol–M′ junction. Secondly, in the STM configuration, intermolecular electron hopping does not significantly enhance the junction transport characteristics. Thirdly, the symmetric behaviour of the *I–V* curves obtained, despite the different metal–molecule contacts, indicates that the molecule is simply an amphiphilic electron-donating wire and not a molecular diode with strong rectifying characteristics. Finally, the conductance values obtained from the amine/TMS-contacted OPE described here are of the same order of magnitude as thiol anchored OPEs, making them attractive alternatives to the more conventionally used thiol-contacting chemistry for OPE molecular wires.

Keywords: conducting materials · Langmuir–Blodgett films · molecular wires · thin layers

Introduction

The development of ever smaller sized electronic devices has turned interest toward organic molecules as potential circuit components, such as conductors, rectifiers, transistors and logic gates.[1–3] To understand their electrical behaviour direct current-voltage (*I–V*) measurements are a requirement for molecules arranged into metal-molecule-metal junctions. There are now a number of methods capable of achieving this feat and they include mechanical break junctions,[4,5] nanopores,[6,7] cross-wire junctions,[8] scanning tunnelling microscopy (STM)[9–13] or conducting atomic force microscopy (c-AFM).[14–16] Molecular conductance values obtained from such devices, depend not only on the inherent molecular features, but also on other important parameters, such as the metal–molecule contact. Often, small variations in the nature or characteristics of the metal–molecule con-

[a] G. Pera, Dr. S. Martín, L. M. Ballesteros, Dr. P. Cea
Departamento de Química Orgánica y Química Física
Facultad de Ciencias
Universidad de Zaragoza, 50009 (Spain)
E-mail: pilarcea@unizar.es

[b] G. Pera, Dr. S. Martín, L. M. Ballesteros, Dr. P. Cea
Instituto de Nanociencia de Aragón (INA)
edificio I+D+I, C/Mariano Esquilor s/n Campus Rio Ebro
50018, Zaragoza (Spain)

[c] A. J. Hope, Prof. P. J. Low
Department of Chemistry
University of Durham
Durham DH1 3 LE (UK)

[d] Prof. R. J. Nichols
Department of Chemistry
University of Liverpool
Crown Street, Liverpool, L69 7ZD (UK)

Supporting information for this article is available on the WWW under http://dx.doi.org/10.1002/chem.201001181.

tact can have a pronounced effect on charge transport in the junction.[17,18]

The Langmuir–Blodgett (LB) technique is an effective tool for transferring well-ordered molecular films at the air–water interface onto a solid support, permitting a degree of control over the molecule–surface interaction or contact, as it is applicable for forming both chemisorbed and physisorbed films.[19] Therefore, the use of the LB metal–organic assembly technologies provides diverse opportunities for the exploration of different metal–molecule contacts that, so far, have been limited to a few interfaces formed by the traditional self-assembly (SA) method. The thiol moiety has been used extensively to attach molecules to gold surfaces using such SA methods. However, the shortcomings of the Au–S attachment have become apparent in recent years.[20] For example, the Au–S bond is mobile at room temperatures giving rise to device instabilities such as stochastic switching.[21–23] Measurements at the single molecule level have demonstrated that Au–S contacts have multiple contact values, which depend on the nature of the coordination bond between the sulphur and the gold contact; moreover, these contacts have shown unexpectedly high resistance.[24] To overcome these problems it is clear that alternative contact chemistries should be intensively investigated and LB technologies provide a powerful platform for achieving this.

To the best of our knowledge, trimethylsilane (TMS) has not yet been employed in metal–molecule–metal junctions studies, although oligothiophene derivatives[25] and n-alkanes[26] bearing the TMS group have been shown to form long-range and highly-stable self-assembled monolayers onto reconstructed Au(111). Herein we examine the role of this unexplored linker by measuring the conductivity of both single molecules (SMC) and assemblies of molecules positioned onto gold substrates by the LB technique. Thus, the *I–V* response of an asymmetric oligomeric phenylene ethynylene (OPE) derivative (TMS-OPE-NH_2), functionalised at one of the terminal position with a TMS group

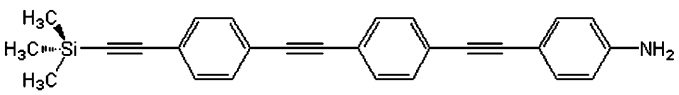

TMS–OPE–NH_2

linked to the OPE core through a C≡C triple bond, and further functionalised with an amine binding group, is presented here. TMS-OPE-NH_2 lacks the supporting, but insulating, alkyl chain ("tail"), which has been included in the molecular skeleton of OPE derivatives assembled into films by the LB technique in previous studies.[27–31] Removing the alkyl tail allows a direct contact between the conjugated skeleton of the molecule through functional groups to the gold substrate and the STM tip, thereby improving the electrical transport through these molecular assemblies.[13,32–36]

Results and Discussion

Characterisation of Langmuir and Langmuir–Blodgett films: Figure 1a shows the representative surface pressure (π–A) and surface potential (ΔV–A) isotherms of TMS-OPE-NH_2 on a water subphase. The π–A isotherm is characterised by

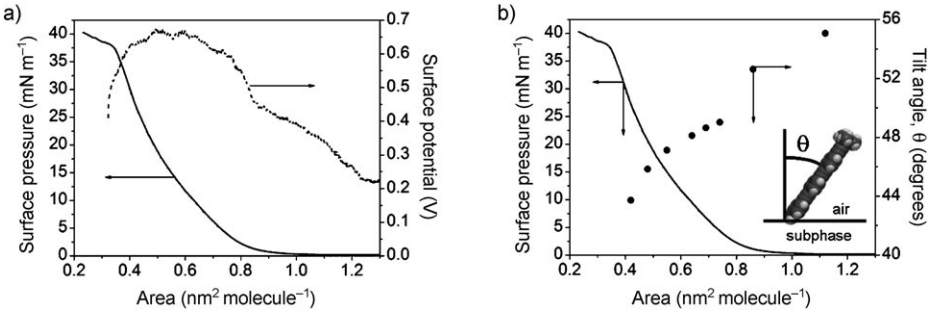

Figure 1. a) π–A (solid line) and ΔV–A (dashed line) isotherms of TMS-OPE-NH_2 on water; b) π–A isotherm (left) and tilt angle, θ, formed by the normal to the surface and the transition dipole moment of the molecule (right) versus the area per molecule.

a zero surface pressure in the 1.3–0.90 nm^2 $molecule^{-1}$ range, featuring a lift-off at approximately 0.90 nm^2 $molecule^{-1}$ followed by an increase of the surface pressure upon compression. Changes in the slope reveal a progressive orientation and/or reorientation of the molecules at the interface during compression. ΔV–A isotherms are well-known to anticipate the phase changes, showing deviations a few $Å^2$ before they are detected in the π–A isotherms.[37] The sudden decrease of ΔV values at approximately 0.47 nm^2 upon compression is especially noteworthy and is consistent with a collapse of the monolayer, in which the dipole moments are randomly distributed in a three-dimensional arrangement of TMS-OPE-NH_2 molecules. Such a collapse can also be observed at slightly lower areas per molecule in the π–A isotherm.

Molecular organisation in Langmuir films was investigated in situ by UV/Vis reflection spectroscopy through the reflection of unpolarised light under normal incidence. Normalised reflection spectra ($\Delta R_n = \Delta R \cdot$Area per molecule, in which ΔR is the reflection) recorded at different values of the surface pressure are illustrated in Figure 2. As can be observed, the intensity of the band at $\lambda = 310$ nm, characteristic of the phenylene-ethynylene moiety,[38] decreases considerably upon compression. This phenomenon is indicative of a gradual decrease of the tilt angle formed by the normal to the surface and the dipole transition moment of the molecules revealing a progressive orientation of the molecules at the interface upon compression.[39] In addition, the band has a marked blue-shift of approximately 33 nm with respect to

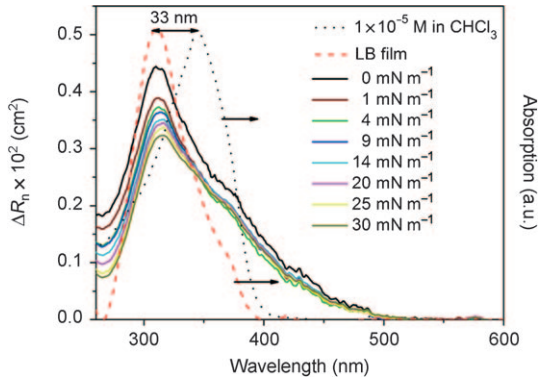

Figure 2. Left: Normalised reflection spectra, ΔR_n, of TMS-OPE-NH_2 spread onto water recorded at the indicated surface pressures (solid lines). Right: The black dotted line shows the UV/Vis absorption spectrum of TMS-OPE-NH_2 1×10^{-5} M in chloroform solution and the dashed red line shows the UV/Vis spectrum of a one-layer LB film.

the absorption band in solution (Figure 2, dotted line), attributable to the formation of H-aggregates (side by side alignment of transition dipole moments of dyes).[40] There is a small red shift of 4 nm of the maximum wavelength of the normalised reflection spectra upon compression, which could be attributed to a less polar environment when the surface pressure increases. In keeping with this suggestion, a bathochromic shift of 2 nm in this characteristic absorption band of TMS-OPE-NH_2 is observed in CCl_4 solution (non-polar) compared to the $CHCl_3$ solution (polar). The angle, θ, defined as the angle formed by the normal to the surface and the transition dipole moment of the molecule (inset of Figure 1b) can be calculated from the normalised reflection spectra.[39] The variation of this angle upon compression is shown in Figure 1b. Notably, the spectra recorded in the gas phase of the isotherm (1.3–0.9 nm^2) show a large dispersion in the angle values, probably as a result of the presence of non-uniform domains in the monolayer underneath the fibre-optic detector, which produce significant fluctuations in the signal.[41] However, as soon as the isotherm takes off, all the spectra follow a logical evolution.

Brewster angle microscopy (BAM) investigations were made during the compression of the Langmuir film and gave further insight into the formation of the monolayer (Figure 3). At a surface pressure of 5 mN m^{-1} the monolayer features some domains, which coalesce as the surface pressure increases. This phenomenon is accompanied by a certain increase in the brightness of the images indicative of a gradual tilt of the molecules as confirmed by the reflection experiments (Figures 1b and 2). At 15 mN m^{-1} a much more homogeneous film can be observed, although some less well covered regions can still be seen in the BAM images. At 20 mN m^{-1} a highly homogeneous monolayer is formed.

Langmuir monolayers were transferred onto solid substrates, initially immersed in the subphase by the vertical dipping method at a surface pressure of 20 mN m^{-1}, to form one-layer LB films. The transfer ratio calculated by the trough software was 1. This deposition rate was also assessed using a quartz crystal microbalance (QCM). Thus, the frequency change (Δf) for a QCM quartz resonator before and after the deposition process was determined. Using the Sauerbrey equation [Eq. (1)]:[42]

$$\Delta f = -\frac{2f_0^2\Delta m}{A\rho_q^{1/2}\mu_q^{1/2}} \quad (1)$$

for which f_0 is the fundamental resonant frequency of 5 MHz, Δm(g) is the mass change, A is the electrode area, ρ_q is the density of the quartz (2.65 g cm^{-3}), and μ_q is the shear module ($2.95\cdot10^{11}$ dyn cm^{-2}), and TMS-OPE-NH_2 molecular weight (389 g mol^{-1}), the surface coverage (Γ) is $3.6\cdot10^{-10}$ mol cm^{-2}, which is in excellent agreement with the estimated value for the saturated surface coverage, $3.5\cdot10^{-10}$ mol cm^{-2}, determined from the molecular area of TMS-OPE-NH_2 at the air–water interface at a surface pressure of 20 mN m^{-1}.

XPS experiments revealed that under these transference process conditions, the amine group of the OPE derivative bonds directly to the gold substrate giving the following schematic structure: Au-NH_2-OPE-TMS. Figure 4 shows the XPS scans of the N 1s region in LB films, as well as in the powder. The XPS spectrum of a solid sample of NH_2-OPE-TMS powder shows a peak at 400.9 eV, corresponding to a free amine group (Figure 4a, top). In contrast, a peak corresponding to N atoms in the LB film, with a binding energy of 399.2 eV, is observed in the XPS spectrum of the LB

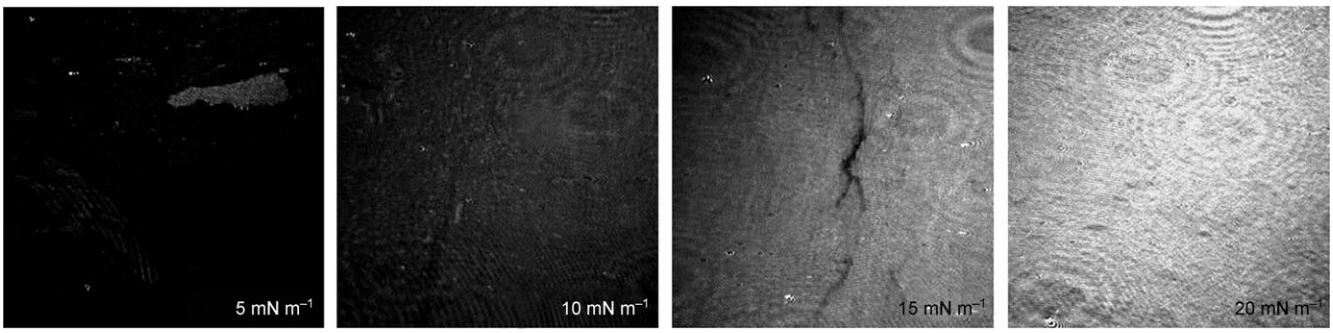

Figure 3. The Brewster angle microscopy (BAM) images of the Langmuir films, at the indicated surface pressures, for TMS-OPE-NH_2 on water. The field of view along the x axis for the BAM images is 3000 μm.

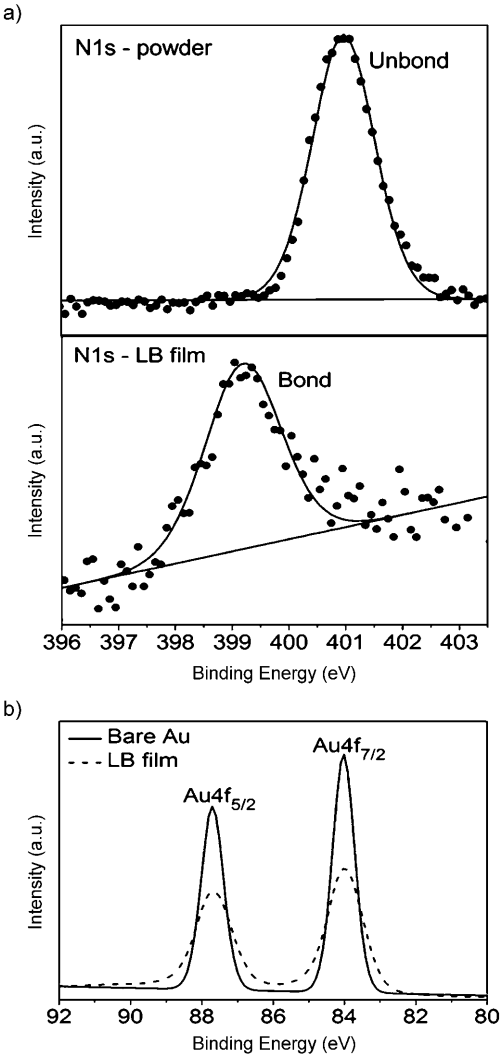

Figure 4. a) XPS spectra of N1s region for the powder (top) and for a one-layer LB film deposited at 20 mN m^{-1} onto a gold substrate (bottom), b) XPS spectra of the Au4f region for bare Au substrate and a Au substrate covered by one monolayer of NH_2-OPE-TMS.

films (Figure 4a, bottom). These observations are consistent with the amine group being adsorbed onto the gold surface in the LB films.[43]

The lack of alkyl chains in this OPE derivative, commonly used to stabilise LB films by promoting strong van der Waals interactions between neighbouring molecules, and the presence of the trimethylsilane group opens the question of whether the LB films of TMS-OPE-NH_2 prepared here are well packed, forming an uniform and homogeneous monolayer, or not. The morphology of the films transferred onto freshly cleaved mica substrates can be evaluated by AFM imaging.[44] The image and section analysis profile of a one-layer LB film are shown in Figure 5, revealing a homogeneous surface (the film roughness, calculated in terms of the root mean squared (RMS), is quite low, ≈0.05 nm), in which the mica is wholly covered by the monolayer (lower surface pressures of transference show the presence of holes or incompletely covered surfaces).

A UV/Vis spectrum of a one-layer LB film of TMS-OPE-NH_2 on quartz was also obtained (dashed red line in Figure 2). The spectrum is similar in profile to the reflection spectra obtained at the air–water interface upon compression, with a maximum absorption feature at $\lambda = 310$ nm. This similarity in both spectra indicates that the 2D H-aggregates formed at the air–water interface are preserved in LB films.

Electrochemical electron transfer currents at electrodes under controlled potential provide an indirect measure of defect densities in thin films[45] and can be conveniently studied by cyclic voltammetry for the film coated electrodes. Cyclic voltammograms (CVs) obtained from aqueous solutions containing 1 mM $K_3[Fe(CN)_6]$ and 0.1 M KCl for a bare gold and for a gold working electrode modified by a one-layer LB film deposited at 20 mN m^{-1} are shown in Figure 6. The electrochemical response of a bare gold electrode exhibits a clear voltammetric wave for ferricyanide. The absence of these peaks for the electrode modified by the LB film indicates a large passivation of the electrode and a lack (or low density) of holes or defects in the monolayer. This indicates that TMS-OPE-NH_2 yields high-quality films.

STM for *I–V* measurements: The electrical properties of a one-layer LB film deposited onto gold substrates initially immersed in the subphase at 20 mN m^{-1} were investigated using a STM. Current-voltage (*I–V*) curves were recorded and averaged from multiple (525) scans at different locations on the substrate and using different samples to ensure the reproducibility and reliability of the measurements. Nevertheless, the vertical position of the STM tip with respect to the monolayer is a determining factor in the recorded electrical properties of the assembled molecules. If the STM tip is not in contact with the monolayer, a gap exists between tip and monolayer. Alternatively, at close enough tip proximities the STM tip will penetrate the monolayer. In such circumstances it is difficult to know how far the tip penetrates and thus what portions of the molecules contrib-

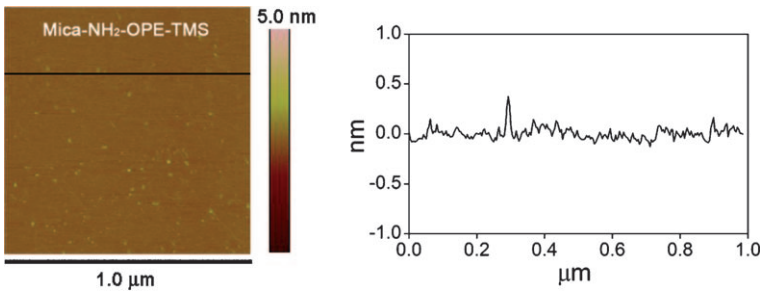

Figure 5. AFM image (left) and section analysis profile (right) of a one-layer LB film transferred at 20 mN m^{-1} onto freshly cleaved mica.

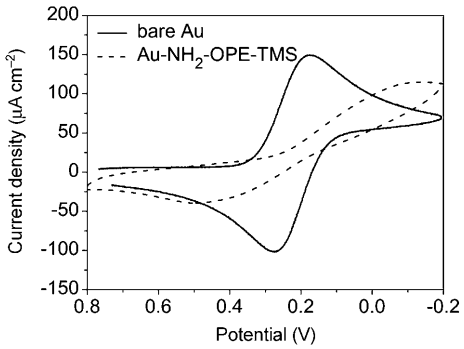

Figure 6. Cyclic voltammogram (CV) of a one-layer LB film of TMS-OPE-NH_2 deposited on a gold electrode at 20 mN m^{-1}(dotted line). CVs were recorded by immersing the LB film in aqueous solutions of 1 mM $K_3[Fe(CN)_6]$ and 0.1 M KCl using a scan rate of 0.05 V s^{-1} at 20 °C. A Ag|AgCl|saturated KCl reference electrode was employed and the counter electrode was a Pt sheet. The solid line shows the response of a bare gold electrode in the same solution and conditions.

ute to the current. Therefore, it is necessary to know, before recording the *I–V* curves, both the thickness of the monolayer and the tip-substrate distance (s) in order to position the STM tip in a defined manner above the monolayer and so avoid either penetration of the STM tip into the film or the existence of a substantial gap between the STM tip and the monolayer. The thickness of the monolayer (1.49 ± 0.04) nm, was determined by using the attenuation of the Au 4f signal in the XPS spectra (Figure 4b) as explained in the Experimental Section. This thickness gives an average tilt angle for the molecules in the LB film of 48° from the surface normal, taking in account the molecule length (2.23 nm) estimated by molecular modelling. This value is in good agreement with the tilt angle obtained from reflection spectroscopy at the air–water interface (46°) at a surface pressure of 20 mN m^{-1} (Figure 1b). The tip-substrate distance (s) was measured making use of a careful calibration where the set-point parameters ($I_0 \equiv$ "set-point current" and $U_t \equiv$ "tip bias") can be converted to an absolute gap separation (s), as follows. $I(s)$ scans (exponential dependence of current (I) on distance (s)), which display a monotonic exponential decrease of the tunnelling current (no wire formation) as the tip is retracted were recorded at regular intervals during the measurements. These monotonic exponential decay curves were then plotted as $\ln(I)$ versus s. Averaging the slope of the corresponding $d\ln(I)/ds$ curves, ($d\ln(I)/ds$ was typically in the order of 7.59 ± 0.88 nm^{-1}), and assuming that the conductance at the point where metal-tip contact occurs is the conductance quantum G_0 ($G_0 = 2e^2/h \approx 77.4$ μS), provide the basis for an estimation of the gap separation (tip-substrate distance) at a given current according to Equation (2).

$$s = \frac{\ln(G_0 \times U_t/I_0)}{d\ln(I)/ds} \qquad (2)$$

I–V curves for a one-layer TMS-OPE-NH_2 LB film using several set-point parameters ($U_t = 0.6$ V and $I_0 = 0.3$, 0.5 and 1.0 nA), which give different initial tip-substrate distances (1.57, 1.50 and 1.42 nm) according to Equation (2), are shown in Figure 7a. In agreement with the thickness of the monolayer, 1.49 ± 0.04 nm, at 0.5 nA and 0.6 V ($s = 1.50$ nm) the tip is positioned just above the monolayer. Meanwhile, for 1.0 nA ($s = 1.41$ nm) the tip penetrates inside the monolayer (conductance and rectification increase) and for 0.3 nA ($s = 1.57$ nm) there is a notable gap between the tip and the LB film (junction conductance decreases).

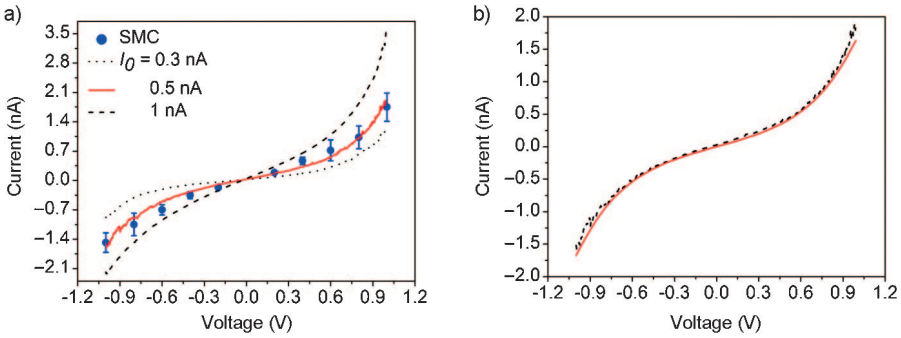

Figure 7. a) *I–V* curves of a one-layer LB film of TMS-OPE-NH_2 transferred onto Au(111) at 20 mN m^{-1} using several set-point parameters: 0.3 nA ($s = 1.57$ nm) (black dashed line); 0.5 nA ($s = 1.50$ nm) (red solid line); and 1.0 nA ($s = 1.42$ nm) (black dotted line). An *I–V* curve constructed from single-molecule conductance values obtained by using the $I(s)$ method is also shown (blue circles). The error bars represent the standard deviation. $U_t = 0.6$ V. b) *I–V* curve of a one-layer LB film of TMS-OPE-NH_2 at 0.5 nA (dashed line) and fitting according to the Simmons equation, $\Phi = 0.68$ eV, $\alpha = 0.42$ (red solid line).

In addition to results from the conductance studies for the monolayer covered surfaces, Figure 7a also shows an *I–V* curve constructed from single molecule conductance (SMC) values for TMS-OPE-NH_2 obtained by using the $I(s)$ method at 10 different bias voltage values. The $I(s)$ method developed by Haiss et al. has been widely used to determine the single-molecule conductance of several compounds[10,24,46] and description of it can be found in the literature.[9,24,47] The SMC-curve coincides with the *I–V* curve obtained for the LB film covered surface recorded at 0.5 nA setpoint current. These results indicate that with these parameters the STM tip is located directly above the LB film and electronically coupled to a single molecule. Under such conditions the STM tip probes the conductance of a single TMS-OPE-NH_2 molecule embedded in the LB film by using the trimethylsilane group to form contact with the gold STM tip. There is similarity between both *I–V* curves, de-

spite the different molecular surroundings in the two cases. In the LB film case the molecule is packed together with neighbouring TMS-OPE-NH_2 molecules, whereas no such neighbours exist for the SMC determinations. This indicates that for the LB film intermolecular electron hopping does not significantly enhance the junction transport characteristics and that the presence of neighbouring π systems does not greatly influence the STM determined molecular conductance. From this observation it is concluded that the existence of intermolecular interactions and 2D aggregates (H-aggregates) in the LB films (as demonstrated by UV/Vis spectroscopy) does not have a significant impact on the junction electrical characteristics.

The *I–V* response for the SMC-curve and for the *I–V* curve obtained at 0.5 nA is close to ohmic between bias voltages of −0.6 to +0.6 V giving a molecule conductance value of approximately $1.2\times10^{-5}\ G_0$. This value is the same order of magnitude as the conductance value obtained for other OPE derivatives using thiols as anchoring groups ($1.8\times10^{-5}\ G_0$).[48,49] Therefore, it is concluded that both the amino and trimethylsilane groups are alternative linkers that provide electronic coupling between the electrodes and the molecule which is essentially as efficient as that through thiols. However, outside the −0.6 to +0.6 voltage range the response deviates from linearity showing a sigmoidal behaviour over the full voltage region. In addition, the SMC-curve and the *I–V* curve at 0.5 nA set-point current are nearly symmetrical despite the asymmetry of the molecule. This implies that its behaviour is like that of a molecular wire for which the molecule is simply an amphiphilic electron-donating wire, as has been previously reported for similar OPE derivatives,[35,50–52] and does not behave like a molecular diode with strong rectifying characteristic produced by the asymmetric molecular junction.

The *I–V* curves characteristics indicate that the mechanism of transport through these metal-molecule-metal junctions is non-resonant tunnelling. A widely applied tunnelling model that can be used for comparison with the experimental *I–V* data is the Simmons model.[53] In this model, the current *I* is given by Equation (3),

$$I=\frac{Ae}{4\pi^2\hbar s^2}\left\{\left(\Phi-\frac{eV}{2}\right)\exp\left[-\frac{2(2m)^{1/2}}{\hbar}\alpha\left(\Phi-\frac{eV}{2}\right)^{1/2}s\right]-\left(\Phi+\frac{eV}{2}\right)\exp\left[-\frac{2(2m)^{1/2}}{\hbar}\alpha\left(\Phi+\frac{eV}{2}\right)^{1/2}s\right]\right\} \quad (3)$$

for which *V* is the applied potential, *A* is the contact area of the molecule with the tip (0.48 nm^2 in concordance with the isotherm shown in the Figure 2 at the surface pressure of 20 $mN\,m^{-1}$and since the STM tip is electronically coupled to a single molecule in the LB films according to Figure 7a), *s* is the width of the tunnelling barrier which was assumed to be the through-bond distance between the end groups in OPE molecular wire as calculated with a molecular modelling program (2.23 nm), Φ is the effective barrier height of the tunnelling junction (relative to the Fermi level of the Au), α is related to the effective mass of the tunnelling electron and *m* and *e* represent the mass and the charge of an electron. To fit the *I–V* data in Figure 7b, Φ and α are the fit parameters. A good agreement between the data and the model is obtained with $\Phi=0.68$ eV, and $\alpha=0.42$. In spite of having molecular "asymmetry", this effective barrier height is slightly higher than that obtained by Lu et al.[13] for a symmetric OPE with amine groups in both ends ($\Phi\approx0.60$ eV). These collected electrical measurements indicate that the TMS can be used as an effective anchoring group in metal–molecule–metal junctions without significant impairment of transport through the molecular wire, when bench marked against thiol end-groups. This shows that TMS is an efficient linker for electron transport through molecular junctions.

Conclusion

An antisymmetric OPE derivative, with an amine group on one end and a trimethylsilane group linked to the aromatic ring through a triple bond at the other, has been synthesised and assembled into well-packed monolayer films by means of the Langmuir–Blodgett technique. Langmuir films were prepared at the air–water interface and characterised by π–*A* and Δ*V*–*A* isotherms, which demonstrate that this molecule can form true monolayers at the air–water interface. Analysis of UV/Vis reflection spectra revealed the formation of two dimensional H-aggregates and a gradual transition of the molecules to a more vertical position upon compression. These monomolecular films were transferred undisturbed onto solid substrates with a transfer ratio close to 1 with a Au-NH_2-OPE-TMS structure as demonstrated by XPS. Cyclic voltammograms showed the absence (or low density) of holes or defects in the monolayers of this molecule despite of the absence of alkyl chains commonly used to stabilise LB films. Electrical characteristics of the LB films on gold substrates were determined from *I–V* curves, with a gold STM tip positioned sufficiently above the monolayer as determined from calibration of the tip–substrate distance and determination of the thickness of the LB film. *I–V* curves recorded at different set-point parameters were compared with those constructed from single-molecule conductance values obtained by using the *I*(*s*) technique. The coincidence between both curves shows that the conductance of a single TMS-OPE-NH_2 molecule embedded in the LB film is probed. Importantly, it is concluded that TMS is an alternative anchoring group, which provides effective electronic coupling at metal–molecule contacts. Finally, analysis of the *I–V* curve showed a non-resonant tunnelling mechanism with a symmetrical response indicative of non-rectifying molecular wire-like characteristics.

Experimental Section

Film fabrication: 4-[4-{4-(Trimethylsilylethynyl)phenylethynyl}phenylethynyl]aniline (TMS-OPE-NH_2) was prepared as described in the Supporting Information. A Nima Teflon trough with dimensions $720\times 100\,mm^2$ housed in a constant temperature ($20\pm1\,°C$) clean room was used to prepare the films. The surface pressure (π) of the monolayers was measured by using a Wilhelmy paper plate pressure sensor. Ultrapure Milli-pore Milli-Q water (resistivity 18.2 MΩ cm) was used as subphase. The spreading solutions (1×10^{-5} M) in TMS-OPE-NH_2 were prepared in chloroform (HPLC grade, 99.9% purchased from Sigma). To construct the Langmuir films, the solution was spread using a Hamilton micro-syringe held very close to the aqueous surface, allowing the surface pressure to return to a value as close as possible to zero between each addition. The spreading solvent was allowed to completely evaporate over a period of at least 15 min before compression of the Langmuir film at a constant sweeping speed of $0.02\,nm^2\,molecule^{-1}\,min^{-1}$. Each compression isotherm was recorded at least three times to ensure the reproducibility of the results so obtained. Surface potential measurements were carried out using a Kelvin Probe provided by Nanofilm Technologie GmbH, Göttingen, Germany. During monolayer compression, π–A and ΔV–A isotherms were recorded simultaneously. Meanwhile, a commercial UV/Vis reflection spectrophotometer, with a light source FiberLight DTM 6/50 and an absolute wavelength accuracy <0.3 nm and a resolution (Raylight-criterion) >3 nm, was used to obtain the reflection spectra of the Langmuir films upon compression.[39] A commercial mini-Brewster Angle Microscope (mini-BAM), from Nanofilm Technologie, was employed for the direct visualisation of the monolayers at the air/water interface.

The films were deposited at a constant surface pressure by the vertical dipping method with a dipping speed of $0.6\,cm\,min^{-1}$. The solid substrates used to support the LB films were quartz, mica, and gold. UV/Vis spectra were acquired on a Varian Cary 50 spectrophotometer. Atomic Force Microscopy (AFM) experiments were performed by means of a Multimode extended microscope with Nanoscope IIIA electronics from Digital Instruments, using the tapping mode. The data were collected with a silicon cantilever provided by Nanoworld, with a force constant of 42 mN and operating at a resonant frequency of 285 kHz. The images were collected with a scan rate of 1 Hz, an amplitude set point lower than 1 V, and in ambient air conditions.

Cyclic voltammetry (CV) experiments were completed by using an electrochemical cell containing three electrodes. The working electrode consisted of either a gold electrode or a gold substrate with the deposited LB film, the counter electrode was a platinum sheet, and the reference electrode was Ag | AgCl | saturated KCl.

The XPS spectra of LB films on Au substrates were recorded using a Kratos AXIS ultra DLD spectrometer with a monochromatic $Al_{K\alpha}$ X-ray source (1486.6 eV) employing a pass energy of 20 eV at photoelectron take-off angles of 90° with respect to the sample plane. Surface charging was compensated by referencing the adventitious Au($4f_{7/2}$) peak at 84.0 eV. The thickness of LB films on the gold substrates was estimated using the attenuation of the Au 4f signal from the substrate according to: $I_{LB\,film} = I_{substrate}\exp(-d/\lambda\sin\theta)$, where d is the film thickness, $I_{LB\,film}$ and $I_{substrate}$ are the average of the intensities of the Au $4f_{5/2}$ and Au $4f_{7/2}$ peaks attenuated by the LB film and from clean gold, respectively, θ is the photoelectron take-off angle, and $\lambda = 4.2\pm0.1$ nm[54] is the effective attenuation length of the photoelectron.

An Agilent STM running Picoscan 4.19 Software was used for all measurements of molecular conductance. The tip potential is referred to as U_t. STM tips were freshly prepared for each experiment by etching of a 0.25 mm Au wire (99.99%) in a mixture of HCl (50%) and ethanol (50%) at +2.4 V. Gold films employed as substrates were purchased from Arrandee, Schroeer, Germany. These were flame-annealed at approximately 800–1000 °C with a Bunsen burner immediately prior to use to prepare atomically flat Au(111) terraces.[55]

Acknowledgements

G.P., L.M.B., S.M. and P.C. are grateful for financial assistance from the Ministerio de Ciencia e Innovación from Spain and fondos FEDER in the framework of project CTQ2009–13024. P.J.L holds an EPSRC Leadership Fellowship. R.J.N. thanks EPSRC for funding. G.P. gratefully acknowledges the award of a FPU fellowship from MEC. S. M acknowledges his Juan de la Cierva position from Ministerio de Ciencia e Innovación (Spain) and L.M.B acknowledges her grant from Banco Santander. We are also grateful to Dr. Jordi Díaz from the University of Barcelona and Dr. Guillermo Antorrena from Instituto de Nanociencia de Aragón for their help with the AFM and XPS measurements, respectively.

[1] D. Nilsson, S. Watcharinyaron, M. Eng, L. Li, E. Moons, L. Johanson, M. Zharnikov, A. Shaporenko, B. Albinsson, J. Martensson, *Langmuir* **2007**, *23*, 6170–6181.
[2] A. M. Rawlett, T. J. Hopson, I. Amlani, R. Zhang, J. Tresek, L. A. Nagahara, R. K. Tsui, H. Goronkin, *Nanotechnology* **2003**, *14*, 377–384.
[3] U. H. F. Bunz, *Adv. Polym. Sci.* **2005**, *177*, 1–52.
[4] M. A. Reed, C. Zhou, C. J. Muller, T. P. Burgin, J. M. Tour, *Science* **1997**, *278*, 252–254.
[5] A. Salomon, D. Cahen, S. Lindsay, J. Tomfohr, C. B. Engelkes, D. D. Frisbie, *Adv. Mater.* **2003**, *15*, 1881–1890.
[6] J. Chen, M. A. Reed, A. M. Rawlett, J. M. Tour, *Science* **1999**, *286*, 1550–1552.
[7] E. A. Osorio, K. O'Neill, M. Wegewijs, N. Stuhr-Hansen, J. Paaske, T. Bjornholm, H. S. J. van der Zant, *Nano Lett.* **2007**, *7*, 3336–3342.
[8] B. Kim, J. M. Beebe, C. Olivier, S. Rigaut, D. Touchard, J. G. Kushmerick, X. Y. Zhu, C. D. Frisbie, *J. Phys. Chem. C* **2007**, *111*, 7521–7526.
[9] W. Haiss, H. van Zalinge, S. J. Higgings, D. Bethell, H. Höbenreich, D. J. Schiffrin, R. J. Nichols, *J. Am. Chem. Soc.* **2003**, *125*, 15294–15295.
[10] G. Sedghi, K. Sawada, L. J. Esdaile, M. Hoffmann, H. L. Anderson, D. Bethell, W. Haiss, S. J. Higgins, R. J. Nichols, *J. Am. Chem. Soc.* **2008**, *130*, 8582–8583.
[11] A. M. Moore, B. A. Mantooth, Z. J. Donhauser, F. Maya, D. W. Price, Y. Yao, J. M. Tour, P. S. Weiss, *Nano Lett.* **2005**, *5*, 2292–2297.
[12] K. Liu, X. Wang, F. Wang, *ACS Nano* **2008**, *2*, 2315–2323.
[13] Q. Lu, K. Liu, H. Zhang, Z. Du, X. Wang, F. Wang, *ACS Nano* **2009**, *3*, 3861–3868.
[14] X. D. Cui, A. Primak, X. Zarate, J. Tornfohr, O. F. Sankey, A. L. Moore, A. T. Moore, D. Gust, G. Harris, S. M. Lindsay, *Science* **2001**, *294*, 571–574.
[15] B. Kim, J. M. Beebe, Y. Jun, X. Y. Zhu, C. D. Frisbie, *J. Am. Chem. Soc.* **2006**, *128*, 4970–4971.
[16] J. M. Beebe, B. Kim, C. D. Frisbie, J. G. Kushmerick, *ACS Nano* **2008**, *2*, 827–832.
[17] J. M. Beebe, V. B. Engeelkes, L. L. Miller, C. D. Frisbie, *J. Am. Chem. Soc.* **2002**, *124*, 11268–11269.
[18] V. B. Engelkes, J. M. Beebe, C. D. Frisbie, *J. Am. Chem. Soc.* **2004**, *126*, 14287–14296.
[19] S. H. Gyepi-Garbrah, R. Silerova, *Phys. Chem. Chem. Phys.* **2002**, *4*, 3436–3442.
[20] F. Chen, X. Li, J. Hihath, Z. Huang, N. J. J. Tao, *J. Am. Chem. Soc.* **2006**, *128*, 15874–15881.
[21] G. K. Ramachandran, T. J. Hopson, A. M. Rawlett, L. A. Nagahara, A. Primak, S. M. Lindsay, *Science* **2003**, *300*, 1413–1416.
[22] Z. K. Keane, J. W. Ciszek, J. M. Tour, D. Natelson, *Nano Lett.* **2006**, *6*, 1518–1521.
[23] S. Yasuda, S. Yoshida, J. Sasaki, Y. Okutsu, T. Nakamura, A. Taninaka, O. Takeuchi, H. Shigekawa, *J. Am. Chem. Soc.* **2006**, *128*, 7746–7747.
[24] W. Haiss, S. Martin, E. Leary, H. van Zalinge, S. J. Higgins, L. Bouffier, R. J. Nichols, *J. Phys. Chem. C* **2009**, *113*, 5823–5833.
[25] C. Reese, M. E. Roberts, S. R. Parkin, Z. Bao, *Adv. Mater.* **2009**, *21*, 3678–3681.

[26] N. Katsonis, A. Marchenko, S. Taillemite, D. Fichou, G. Chouraqui, C. Aubert, M. M. , *Chem. Eur. J.* **2003**, *9*, 2574–2581.
[27] G. Pera, A. Villares, M. C. López, P. Cea, D. P. Lydon, P. J. Low, *Chem. Mater.* **2007**, *19*, 857–864.
[28] A. Villares, D. P. Lydon, L. Porrès, A. Beeby, P. J. Low, P. Cea, F. M. Royo, *J. Phys. Chem. B* **2007**, *111*, 7201–7209.
[29] Z. X. Tang, R. K. Hicks, R. J. Magyar, S. Tretiak, Y. Gao, H. L. Wang, *Langmuir* **2006**, *22*, 8813–8820.
[30] A. Villares, S. Martin, I. Giner, J. Diaz, D. P. Lydon, P. Low, P. Cea, *Soft Matter* **2008**, *4*, 1508–1514.
[31] A. Villares, D. P. Lydon, B. J. Robinson, G. Ashwell, F. M. Royo, P. J. Low, P. Cea, *Surf. Sci.* **2008**, *602*, 3683–3687.
[32] Z. J. Donhauser, B. A. Mantooth, K. F. Kelly, L. A. Bumm, J. D. Monnell, J. J. Stapleton, D. W. Price Jr, A. M. Rawlett, D. L. Allara, J. M. Tour, P. S. Weiss, *Science* **2001**, *292*, 2303–2307.
[33] R. Huber, M. T. Gonzalez, S. Wu, M. Langer, S. Grunder, V. Horhoiu, M. Mayor, M. R. Bryce, C. S. Wang, R. Jitchati, C. Schonenberger, M. Calame, *J. Am. Chem. Soc.* **2008**, *130*, 1080–1084.
[34] X. Y. Xiao, L. A. Nagahara, A. M. Rawlett, N. J. J. Tao, *J. Am. Chem. Soc.* **2005**, *127*, 9235–9240.
[35] K. Liu, G. Li, X. Wang, F. Wang, *J. Phys. Chem. C* **2008**, *112*, 4342–4349.
[36] A. Villares, G. Pera, S. Martin, R. J. Nichols, D. P. Lydon, L. Applegarth, A. Beeby, P. J. Low, P. Cea, *Chem. Mater.* **2010**, *22*, 2041–2049.
[37] O. N. Oliveira, Jr., C. Bonardi, *Langmuir* **1997**, *13*, 5920–5924.
[38] A. Beeby, K. Findlay, P. J. Low, T. B. Marder, *J. Am. Chem. Soc.* **2002**, *124*, 8280–8284.
[39] P. Cea, S. Martín, A. Villares, D. Möbius, M. C. López, *J. Phys. Chem. B* **2006**, *110*, 963–970.
[40] X. Song, J. Perlstein, D. G. Whitten, *J. Am. Chem. Soc.* **1997**, *119*, 9144–9159.
[41] A. Gil, I. Arístegui, A. Suárez, I. Sández, D. Möbius, *Langmuir* **2002**, *18*, 8527–8534.
[42] G. Sauerbrey, *Z. Phys.* **1959**, *155*, 206–222.
[43] L. Kankate, A. Turchanin, A. Gölzhäuser, *Langmuir* **2009**, *25*, 10435–10438.
[44] M. Haro, B. Giner, C. Lafuente, M. C. López, F. M. Royo, P. Cea, *Langmuir* **2005**, *21*, 2796–2803.
[45] M. D. Porter, T. B. Bright, D. L. Allara, C. E. D. Chidsey, *J. Am. Chem. Soc.* **1987**, *109*, 3559–3568.
[46] C. S. Wang, A. S. Batsanov, M. R. Bryce, S. Martin, R. J. Nichols, S. J. Higgings, V. M. Garcia-Suarez, C. J. Lambert, *J. Am. Chem. Soc.* **2009**, *131*, 15647–15654.
[47] W. Haiss, R. J. Nichols, H. van Zalinge, S. J. Higgins, D. Bethel, D. J. Schiffrin, *Phys. Chem. Chem. Phys.* **2004**, *6*, 4330–4337.
[48] W. Haiss, C. S. Wang, I. Grace, A. S. Batsanov, D. J. Schiffrin, S. J. Higgins, M. R. Bryce, C. J. Lambert, R. J. Nichols, *Nat. Mater.* **2006**, *5*, 995–1002.
[49] N. Weibel, A. Alfred Błaszczyk, C. von Hänisch, M. Mayor, I. Pobelov, T. Wandlowski, F. Chen, N. Tao, *Eur. J. Org. Chem.* **2008**, 136–149.
[50] G. J. Ashwell, B. Urasinska, W. D. Tyrrell, *Phys. Chem. Chem. Phys.* **2006**, *8*, 3314–3319.
[51] A. Villares, D. P. Lydon, P. J. Low, B. J. Robinson, G. J. Ashwell, F. M. Royo, P. Cea, *Chem. Mater.* **2008**, *20*, 258–264.
[52] J. Reichert, R. Ochs, D. Beckmann, H. B. Weber, M. Mayor, H. von Lohneysen, *Phys. Rev. Lett.* **2002**, *88*, 176804.
[53] J. G. Simmons, *J. Appl. Phys.* **1963**, *34*, 1793–1803.
[54] C. D. Bain, G. M. Whitesides, *J. Phys. Chem.* **1989**, *93*, 1670–1673.
[55] W. Haiss, D. Lackey, J. K. Sass, K. H. Besocke, *J. Chem. Phys.* **1991**, *95*, 2193–2196.

Received: May 3, 2010
Published online: October 7, 2010

